A chimeric design of heterospin 2p-3d, 2p-4f, and 2p-3d-4f complexes using a novel family of paramagnetic dissymmetric compartmental

Chimeric design of heterospin 2*p*-3*d*, 2*p*-4*f*, and 2*p*-3*d*-4*f* complexes using a novel family of paramagnetic dissymmetric compartmental ligands

Andrei A. Patrascu, Sergiu Calancea, Matteo Briganti, Stéphane Soriano, Augustin M. Madalan, Rafael A. Allão Cassaro, Andrea Caneschi, Federico Totti,* Maria G. F. Vaz,* and Marius Andruh*

ABSTRACT. End-off bicompartmental ligands bearing a nitronyl-nitroxide arm have been designed for synthesizing various heterospin molecular systems. These ligands can selectively interact with 3d and 4f metal ions, leading to *2p-4f*, *2p-3d*, and *2p-3d-4f* complexes. Our strategy allows, for the first time, the strict control over the nature and number of spin carriers within the same molecular entity. The magnetic properties of the *2p-4f* and *2p-3d-4f* complexes have been investigated and rationalized by theoretical calculations.

[*] Andrei A. Patrascu

Universidade Federal Fluminense, Instituto de Química, Niterói, Rio de Janeiro, Brazil

and Inorganic Chemistry Laboratory, Faculty of Chemistry, University of Bucharest, Str. Dumbrava Rosie nr. 23, 020464-Bucharest, Romania

Prof. Maria G. F. Vaz, Dr. Sergiu Calancea,

Universidade Federal Fluminense, Instituto de Química, Niterói, Rio de Janeiro, Brazil

Matteo Briganti

Universidade Federal Fluminense, Instituto de Química, Niterói, Rio de Janeiro, Brazil

and Department of Chemistry "Ugo Schiff" and INSTM RU University of Florence 50019 Sesto Fiorentino (Italy)

Prof. Andrea Caneschi, Dr. Federico Totti

Department of Chemistry "Ugo Schiff" and INSTM RU University of Florence 50019 Sesto Fiorentino (Italy)

Dr. Stéphane Soriano

Instituto de Física, Universidade Federal Fluminense, Niterói, Rio de Janeiro, Brazil

Dr. Rafael A. Allão Cassaro

Instituto de Química, Universidade Federal do Rio de Janeiro, Rio de Janeiro, Brazil

Dr. Augustin M. Madalan, Prof. Marius Andruh

Inorganic Chemistry Laboratory, Faculty of Chemistry, University of Bucharest, Str. Dumbrava Rosie nr. 23, 020464-Bucharest, Romania

Keywords: nitronyl-nitroxide ligand, Single Molecule Magnets, *ab initio*.

The nitronyl-nitroxide radicals played a very important role in the history of molecular magnetism.[1] These molecules, carrying an unpaired electron delocalized over the two potentially coordinating oxygen atoms, promote relatively strong exchange interactions with paramagnetic metal ions. Most of the heterospin complexes with nitronyl-nitroxide ligands are assembled using *3d* and *4f* metal ions, while *2p-4d* complexes are limited to few examples.[2]

Considering the heterotrispin systems constructed from one radical (nitronyl-nitroxides, tempo derivatives) and two different paramagnetic metal ions, these are even less numerous. The examples reported to date belong to the following families: (i) supramolecular networks, constructed from heterobimetallic coordination polymers and uncoordinated/weakly coordinated radicals;[3] (ii) heterobimetallic *3d−3d′* complexes with the organic radicals acting as ligands;[4] (iii) heterobimetallic *3d−4f* complexes with the organic radicals acting as ligands.[5] The complexes from the last family are obtained by reacting mixtures of hexafluoroacetylacetonates of Cu^{II} and Ln^{III} with the paramagnetic organic ligands. The presence of the hexafluoroacetylacetonato ligands is necessary, since they increase the Lewis acidity of the metal centers, facilitating the coordination of the N-O groups, which are known to have a poor ability to bind metal ions. Although the one-pot procedures can lead to interesting structures, they do not allow a strict control over the nuclearity and topology of the spin carriers within the resulting molecular entities.

Herein, we present an original family of heterotopic end-off compartmental ligands which can selectively interact with *3d* and *4f* metal ions, leading to predictable heterospin complexes. Our strategy relies on the Mannich reaction, which was first employed by Fenton *et al.* to generate dissymmetric bicompartmental ligands.[6] In our case, one compartment is made by the Mannich-base moiety, while the other one is generated by the nitronyl-nitroxide pendant arm (Scheme 1). The phenoxido oxygen atom acts as a bridge when two metal ions are hosted by the compartmental ligand. Employing these ligands, three types of heterospin systems can be obtained: (a) *2p-4f* complexes, with the oxophilic lanthanide ion located into the compartment formed by the phenoxido and nitroxide oxygens; (b) *2p-3d* complexes, with the two

compartments occupied by *3d* metal ions; (c) *2p-3d-4f* complexes, with the *3d* metal ion hosted into the first (ONN') site and the *4f* ion into the second one (OO').

The synthesis of the ligand (HL) starts from 5-bromo-salicylaldehyde which, in the first step, reacts with formaldehyde and the diamine having one secondary and one tertiary amino groups (Mannich reaction).[6] In the next step, the formyl group is transformed into the nitronyl-nitroxide pendant arm, following the standard protocol.[7] The details of the synthesis are presented in the Supporting Information.

The coordination behavior of ligand HL has been checked by reacting it, separately, with $[Dy(hfac)_3(H_2O)_3]$, $[Co(hfac)_2(H_2O)_2]$, and with the equimolar mixture of $[Dy(hfac)_3(H_2O)_3]$ and $[Co(hfac)_2(H_2O)_2]$ (see supporting information). In the first case, we obtained a mononuclear Dy^{III} complex, $[Dy(LH)(hfac)_3]$ **1**, in the second one a homobimetallic complex, $[Co_2L(hfac)_3]$ **2**, and a heterobimetallic complex $[CoDyL(hfac)_4]$ **3**, is assembled in the third case. The crystal structures of the three compounds have been solved (see Table S1 for the crystallographic data), and the purity of the crystalline phases was proved by powder X-Ray diffraction (Figures S1-S3).

The analysis of the three crystals structures (Figure 1) illustrates the expected selectivity of the HL ligand compartments. Indeed, the OO' site binds the strongly oxophilic Dy^{III} ion both in **1** and **3** leaving empty the ONN' site in **1**. In compound **3** the ONN' site hosts the Co^{II} ion. Since the Co^{II} ions do not have a particular preference for O and N donor atoms, they occupy the two compartments in **2**.

The Dy^{III} ion in **1** (Figure 1a) has a coordination number of eight, with a bicapped trigonal prismatic geometry (six oxygen atoms from the three $hfac^-$ ligands, one from the nitroxide group, and one phenoxido oxygen atom), with bond distances ranging between 2.249(4) and 2.432(4) Å. One nitrogen atom, N3, is protonated (the organic molecule acts as a ligand in the zwitterionic form).

The cobalt ions in compound **2** (Figure 1b) fill the two compartments, being bridged by the phenoxido oxygen and by an oxygen atom arising from one $hfac^-$ ligand. Both cobalt ions are hexacoordinated. Co1 shows a slightly distorted octahedral geometry, being coordinated by six oxygen atoms: four of them arise from the two $hfac^-$ ligands (O7 bridges the two metal ions), one from the phenoxido bridge, and one from the nitroxide group, with Co1···O distances varying between 2.041(3) and 2.117(3) Å. The second metal ion, Co2, is coordinated by the nitrogen

atoms from the Mannich moiety of the ligand (Co2 – N3 = 2.172(3), Co2 – N4 = 2.170(3) Å), by two oxygen atoms from the chelating $hfac^-$ ligand (Co2 – O8= 2.044(2), Co2 – O9 = 2.035(3) Å), an oxygen atom from the phenoxido bridge (Co2 – O3 = 1.985(2) Å), and the sixth one from the bridging $hfac^-$ ligand (Co2 – O7= 2.664(1) Å). It is interesting to notice that this distance is much longer than the one involving Co1: Co1 – O7 = 2.117(3) Å. The intramolecular distance between the cobalt ions is Co1···Co2 = 3.373 Å.

The crystal structure of compound **3** validates the rational synthetic strategy towards *2p-3d-4f* complexes using the new ligand (Figure 1c). Indeed, the end-off compartmental ligand interacts selectively with the two metal ions. These are bridged by an oxygen atom from the phenoxido group and by another one arising from one of the $hfac^-$ ligands coordinated to the Dy^{III} ion. The Co^{II} ion is coordinated by one chelating $hfac^-$ ligand (Co1 – O10 = 2.036(6); Co1 – O11 = 2.027(6) Å), two nitrogen atoms (Co1 – N3 = 2.155(7); Co1 – N4 = 2.155(7) Å), one phenoxido oxygen (Co1 - O3 = 2.024(5) Å), and one bridging oxygen atom (Co1 – O8 = 2.490(5) Å). We notice again that one out of the six bonds involving the cobalt ion is significantly longer than the others. The Dy^{III} ion is eight-coordinated by three $hfac^-$ ligands (one out of the six oxygen atoms acts as a bridge), one nitroxide oxygen atom, and the bridging phenoxido oxygen atom, showing a dodecahedral geometry geometry (bond distances range between 2.322(6) and 2.412(5) Å). The intramolecular distance Co1···Dy1 between the metal ions is 3.732 Å. Selected bond distances and angles are collected in Tables S2 and Table S3.

The magnetic properties of compounds **1** and **3** were investigated in the temperature range 2-300 K. The results of the dc measurements are shown in the form of $\chi_M T$ *vs.* T plots in Figure 2. The room temperature values of the $\chi_M T$ product are 14.4 and 17.5 $cm^3mol^{-1}K$ for compounds **1** and **3**, respectively. The found $\chi_M T$ values are very close to the non-interacting spin carriers (14.5 $cm^3mol^{-1}K$) for **1**, and slightly higher for **3** due to the orbital contribution of the magnetic moment of the Co^{II} ion (17.5 $cm^3mol^{-1}K$ *vs.* the theoretical value of 16.4 $cm^3mol^{-1}K$, neglecting the orbital contribution for Co^{II}).

For the mononuclear Dy^{III} complex **1,** on lowering the temperature, $\chi_M T$ decreases continuously to 13.2 $cm^3mol^{-1}K$ at 45 K, then increases slightly up to 13.3 $cm^3mol^{-1}K$ at 14 K and, finally, goes down to 11.2 $cm^3mol^{-1}K$ at 2 K. The high temperature decrease corresponds to the intrinsic magnetism of the Dy^{III} ion with the depopulation of the M_J sublevels of the $^6H_{15/2}$ state. On the contrary, the increase is due to the ferromagnetic interaction between the Dy^{III} ion

and the radical, as confirmed by the *ab initio* calculations. Indeed, a ferromagnetic interaction between the lanthanide and the radical (J = 2.4 cm^{-1}) was computed by CASSCF method (see SI and table S4) with no spin-orbit contributions (SOC),[8] within the Heisenberg model $\hat{\boldsymbol{H}} = -J(\boldsymbol{S}_{Dy}\cdot\boldsymbol{S}_{Rad})$, where $\boldsymbol{S}_{Dy}$=5/2 and $\boldsymbol{S}_{Rad}$ =½. The single ion anisotropy and the energy levels of the Dy^{III} ion were obtained with the CASSCF/CASSI-SO method (see SI). The fundamental Kramers' doublet shows a strong easy-axis anisotropy, g_z = 19.2, while the first excited state is found well separated at 112 cm^{-1} higher in energy (Tables S5 and S6). Using the computed magnetic parameters, the $\chi_M T$ curve was simulated within the Lines' model (red lines in Figure 2).[9] This is an effective exchange coupling model which allows to reproduce the magnetic exchange properties of strongly anisotropic ions. In order to simulate the curve, a ferromagnetic Dy-Rad exchange coupling J_{Lines} = 8.5 cm^{-1} (with an effective $S_{Dy,eff}$ = ½) was employed, in fairly agreement with the computed one. The simulated curve reproduces very well the experimental one, showing the peak around 14 K. Furthermore, from the CASSCF/CASSI-SO results, the $\chi_M T$ *vs* T data of **1** were fitted below 45 K considering $S_{Dy,eff}$ = 1/2 with anisotropic g values for the Dy^{III} ion. The solid green line in Figure 2 shows the best fit using the MagProp routine in the DAVE software suite,[10] with g_{rad} = 2 (fixed), $g_{Dy,x} = g_{Dy,y}$ = 0 (fixed), $g_{Dy,z}$ = 20.1 ± 0.1 and J = 7.9 ± 0.2 cm^{-1}, which is in good agreement with the magnetic exchange coupling used for the simulation.

With respect to the heterobimetallic complex **3**, upon cooling temperature, $\chi_M T$ decreases continuously down to 11.4 cm^{3}mol^{-1}K at around 2 K. Since the depopulation of the crystal-field M_J sublevels occurs simultaneously with possible magnetic exchange interaction and magnetic anisotropy effects, it is very difficult to interpret, even qualitatively, the magnetic behavior of compound **3**. However, *ab initio* calculations have given useful insights. The calculations and the following simulations were performed with the same procedure employed for compound **1** (see SI). The organic radical interacts ferromagnetically both with the Dy^{III} and the Co^{II} ions. Employing the Heisenberg spin Hamiltonian $\hat{\boldsymbol{H}} = -J_1(\boldsymbol{S}_{Dy}\cdot\boldsymbol{S}_{Rad}) - J_2(\boldsymbol{S}_{Co}\cdot\boldsymbol{S}_{Rad}) - J_3(\boldsymbol{S}_{Dy}\cdot\boldsymbol{S}_{Co})$ with S_{Dy}=5/2, S_{Co}=2, and S_{Rad} =½, J_1 = 0.78 cm^{-1} and J_2 = 0.12 cm^{-1} were found at the *CASSCF* level, while for J_3 the limited hardware resources available prevented its calculation. The reduction of J_1 passing from **1** to **3** can be explained by the less efficient overlap between the radical π*(NO) orbital and the dysprosium *f* orbitals: indeed, in **1** the π*(NO) orbital interacts via σ interaction with an f_0-like orbital while in **3** it interacts more efficiently with an f_1-like orbital via π

interaction. The variation of the Dy-O(2)-N(2)-C_π dihedral angle from 75.9° to 61.7° is claimed as the main reason of the increase of the anti-ferromagnetic contributions (see Figure S4 and Table S2-3).[8]

Regarding the single ion properties, Dy^{III} and Co^{II} ions present strong easy axis anisotropy of their own ground Kramers' doublets, with g_z factors of 19.8 and 6.7 respectively (Table S7). The first excited doublet of the Dy^{III} ion is at 140 cm^{-1} while the one of the Co^{II} ion at 132 cm^{-1} (Table S5). The computation of single ion anisotropies allowed the simulation of the $\chi_M T$ data still within the Lines' model. In order to reproduce the shape of the curve, an antiferromagnetic interaction between the lanthanide and the transition metal ions is needed to be imposed. The best simulation set of values was obtained with J_{Lines1} = 0.9 cm^{-1}, J_{Lines2} = 0.1 cm^{-1}, J_{Lines3} = -2.0 cm^{-1} in very good agreement with the computed values.

The dynamic magnetic properties were investigated by ac magnetic susceptibility measurements. Compound **1** clearly exhibits slow relaxation of magnetization, with frequency dependence for both in-phase (χ') and out-of-phase (χ'') susceptibilities under H = 0 Oe static magnetic field (Figure S5). The increase at low temperatures both for the in-phase and out-of-phase parts is an indication of the occurrence of quantum tunneling of the magnetization (QTM). It is well known that for SMMs and SIMs, QTM occurring at resonance fields, mainly in zero field, can be hampered by an energy barrier caused by a nonzero external field. Therefore, the ac susceptibilities were also measured under a static magnetic field, which shifted the frequency dependence curves to higher temperatures (Figure 3). This behavior is a fingerprint that QTM is occurring at zero magnetic field. For applied field H = 1 kOe, compound **1** exhibits frequency-dependent maxima for both in-phase and out-of-phase susceptibilities (Figure 5). Isothermal ac susceptibility measurements were also performed while varying the ac frequency at different temperatures under 1 kOe applied magnetic field (Figure 4). These data were fitted by a generalized Debye model[11] to extract the relaxation times τ (Table S8) and to obtain the Arrhenius plot (Figure S6). The fit results gave an energy barrier of $\Delta E/k_B$ = 23.5 ± 0.2 K and a pre-exponential factor τ_0 = 9.4 ± 0.5 $.10^{-8}$ s, supporting the presence of a SMM behavior. Such results are in agreement with the *ab initio* computed transition probabilities between the exchange states (Figure 5). Compound **1** has an even number of unpaired electrons and therefore a tunneling splitting, Δ_{tunn}, is expected also in zero field. The computed Δ_{tunn} is of the order of $\sim 10^{-2}$ cm^{-1} and $\sim 10^{-1}$ cm^{-1} for the ground and the first excited pseudo-doublets states (see Table

S9), respectively. The magnitude of the two Δ_{tunn} is large and it would support the presence of strong active QTM between the pseudo-doublets, above all for the first-excited one. However, the pseudo-doublets are the result of the strong exchange coupling (J_{Lines} = 8.5 cm^{-1}) between Dy^{III} and the radical spins, limiting the effective rate of QTM. Therefore, the first excited pseudo-doublet being at 20 cm^{-1} from the ground state and considering that an effective barrier of ~16 cm^{-1} was experimentally found, we can conclude that the whole magnetic behavior of **1** is given by a balance between the exchange coupling driven interaction and the intrinsic tunneling splitting one, where the former is favored. This result is also in agreement with a recent paper showing how the SMM behavior is influenced by the correspondence between large Δ_{tunn} and a relatively strong *J*.[12] In contrast with compound **1**, no frequency dependence was evidenced for the heterobimetallic complex **3** under H = 0 Oe static magnetic field, and only a very weak one was observed when applying a non-zero magnetic field (Figure S7). Even in this case, *ab initio* calculations are in agreement with the experimental findings. Indeed, the computed energy exchange spectrum (see Figure 6) presents four Kramers' doublets in the low lying energy frame (10 cm^{-1}), making several relaxation paths accessible at very low temperatures. Moreover, the QTM is, even in this case, significant due the relatively large transversal *g*-factors of the ground and first Kramers' doublets (see Table S10). Last but not least, the computed easy axis for Dy^{III} and Co^{II} ions are almost orthogonal one each other (they form an angle of 63°) (see Figure 7): in the former case the easy axis is along the direction individuated by the Dy-$O(6)_{hfac}$ bond almost in opposition to the Dy-$O(2)_{Rad}$ one; in the latter, the easy axis points to the N(3)N(4)O(3) face of the Co^{II} octahedron. Such a situation, i.e. lowering the axial character of the resulting exchange states, has been recently claimed as a reason of the relaxation barrier decrease.[13] The results presented herein for **1** and **3** are perfectly in agreement with what reported recently: in order to improve the SMM behavior coupling two strongly anisotropic ions, the two easy axis should be almost parallel or one of the spin unit at least isotropic. In this regards, the improvement of magnetic properties of the 2*p*-3*d*-4*f* complexes could be achieved by tuning the stereochemistry of the Ln^{III} ions (for instance, the hexafluoroacetylacetonato ligands coordinated to Ln^{III} ions could be replaced by different fluoro-beta-diketonato ligands) and by using the isotropic and size-comparable Mn^{II} ion. Moreover, the 2*p*-4*f* exchange coupling could be enhanced by engineering the dihedral Dy-O(2)-N(2)-C_{π} angle.

In conclusion, we have developed an original strategy leading to *2p-3d*, *2p-4f*, and *2p-3d-4f* heterospin complexes, with a strict control over the number and type of spin carriers. The magnetic properties have been successfully rationalized by state-of-art *ab initio* calculations. New other dissymmetric compartmental ligands can be easily synthesized by varying the amines employed in the Mannich reaction. Chiral ligands and, consequently, chiral heterospin complexes can be obtained as well, when chiral amines are chosen. This chemistry is very generous, and we extend it towards other systems containing various pairs of *3d-4f* metal ions. Further work is in progress in our laboratories and will be presented in subsequent papers.

ACKNOWLEDGEMENTS

The authors acknowledge FAPERJ, CAPES, CNPq for the financial support. A. Patrascu and M. Briganti acknowledge FAPERJ – Programa de doutorado Sanduíche Reverso (Project E-26/200.028/2015 and Project E-26/200.104/2016) for the fellowship. We are also grateful to LDRX-UFF and CENAPAD-SP (proj 627) for the use of their facilities. Dr. F. Totti acknowledges the European Research Council Grant MolNanoMas (grant no. 267746), the internationalization program of University of Florence (IFUND2015 n°399 and PIA2013-15) and S. Soriano thanks Conselho Nacional de Desenvolvimento Cientifico e Tecnológico (CNPq).

References

[1] a) A. Caneschi, D. Gatteschi, R. Sessoli, P. Rey, *Acc. Chem. Res*. **1989**, *22*, 392-398; b) S. Demir, I.-R. Jeon, J. R. Long, T. D. Harris, *Coord. Chem. Rev*. **2015**, *289-290*, 149-176; c) A. Caneschi, D. Gatteschi, N. Lalioti, C. Sangregorio, R. Sessoli, G. Venturi, A. Vindigni, A. Rettori, M. G. Pini, M. A. Novak, *Angew. Chem.* **2001**, *113*, 1810–1813; *Angew*. *Chem. Int. Ed.* **2001**, *40*, 1760–1763; d) D. Luneau, P. Rey, *Coord. Chem. Rev*. **2005**, *249*, 2591-2611; e) S. Kaizaki, *Coord. Chem. Rev.* **2006**, *250*, 1804-1818.

[2] See, for example: a) F. Pointillard, K. Bernot. L. Sorace, R. Sessoli, D. Gatteschi, *Dalton Trans*. **2007**, 2689-2695; b) F. Pointillard, K. Bernot, J. Colas, L. Sorace, R. Sessoli, *Inorg. Chim. Acta* **2008**, *361*, 3427-3431; c) Y. Sayama, M. Handa, M. Mikuriya, I. Hiromitsu, K. Kasuga, *Chem. Lett.* **1998**, *27*, 777-778.

[3] a) H. O.Stumpf, L. Ouahab, Y. Pei, D. Grandjean, O. Kahn, *Science* **1993**, *261*, 447-449; b) M. G. F. Vaz, L. M. M. Pinheiro, H. O. Stumpf, A. F. C. Alcântara, S. Gohlen, L. Ouahab, O. Cador, C. Mathonière. O. Kahn, *Chem.-Eur. J*. **1999**, *5*, 1486-1495.

[4] a) A. Caneschi, D. Gatteschi, P. Rey, R. Sessoli, *Chem. Mater*. **1992**, *4*, 204-209 ; b) A. Marvilliers, Y. Pei, J. Cano Boquera, K. E. Vostrikova, C. Paulsen, E. Rivière, J.-P. Audière, T. Mallah, *Chem. Commun*. **1999**, 1951-1952; c) K. E. Vostrikova, D. Luneau, W. Wernsdorfer, P. Rey, M. Verdaguer, *J. Am. Chem. Soc*. **2000**, *122*, 718-719; d) Y.-Z. Zhang, D.-F. Li, R. Clérac, S. M. Holmes, *Polyhedron* **2013**, *64*, 393-398.

[5] a) M. Zhu, Y.-G. Li, Y. Ma, L.-C. Li, D.-Z. Liao, *Inorg. Chem.* **2013**, *52*, 12326-12328; b) L. B. L. Escobar, G. P. Guedes, S. Soriano, N. L. Speziali, A. K. Jordão, A. C. Cunha, V. F. Ferreira, C. Maxim, M. A. Novak, M. Andruh, M. G. F. Vaz, *Inorg. Chem*. **2014**, *53*, 7508-7517; c) M. Zhu, X. Mei, Y. Ma. L. Li, D. Liao, J.-P. Sutter, *Chem. Commun.* **2014**, *50*, 1906-1908; d) M. Zhu, M. Yang, J. Wang, H. Li, L. Li., *Chem.-Asian J.* **2016**, *11*, 1900-1905; e) M. Zhu, L. Li, J.-P. Sutter, *Inorg. Chem. Front.* **2016**, *3*, 994-1003.

[6] J. D. Crane, D. E. Fenton, J. M. Latour, A. J. Smith, *J. Chem. Soc., Dalton Trans*. **1991**, 2979-2887.

[7] a) J. H. Osiecki, E. F. Ullman, *J. Am. Chem. Soc*. **1968**, *90*, 1078; b) E. F. Ullman, L. Call, J. H. Osiecki, *J. Org. Chem*. **1970**, 3623; c) E. F. Ullman, J. H. Osiecki, D. G. B. Boocock, R. Darcy, *J. Am. Chem. Soc*. **1972**, *94*, 7049.

[8] S. G. Reis, M. Briganti, S. Soriano, G. P. Guedes, S. Calancea, C. Tiseanu, M. A. Novak, M. A. del Águila-Sánchez, F. Totti, F. Lopez-Ortiz, M. Andruh, M. G. F. Vaz, *Inorg. Chem.*, **2016**, *55*, 11676-11684

[9] L. F. Chibotaru, L. Ungur, A. Soncini, *Angew. Chem. Int. Ed.*, **2008**, *47*, 4126.

[10] R. T. Azuah, L. R. Kneller, Y. Qiu, P. L. W. Tregenna-Piggott, C. M. Brown, J. R. D. Copley, R. M. DAVE Dimeo: A Comprehensive Software Suite for the Reduction, Visualization, and Analysis of Low Energy Neutron Spectroscopic Data. *J. Res. Natl. Inst. Stan. Technol.* **2009**, *114*, 341−358.

[11] a) K. S. Cole, R. H. Cole, *J. Chem. Phys.* **1941**, *9*, 341; b) M. Costes, J. M. Broto, B. Raquet, H. Rakoto, M. A. Novak, J. P. Sinnecker, S. Soriano, W. S. D. Folly, A. Maignan, V. J. Hardy, *J. Magn. Magn. Mater.* **2005**, *294*, E123.

[12] T. Gupta, M. Faizan Beg, G. Rajaraman, *Inorg. Chem.*, **2016**, *55*, 11201-11215

[13] V. Vieru, T. D. Pasatoiu, L. Ungur, E. Suturina, A. M. Madalan, C. Duhayon, J.-P. Sutter, M. Andruh, L. F. Chibotaru, *Inorg. Chem.*, **2016**, *55*, 12158-1217.

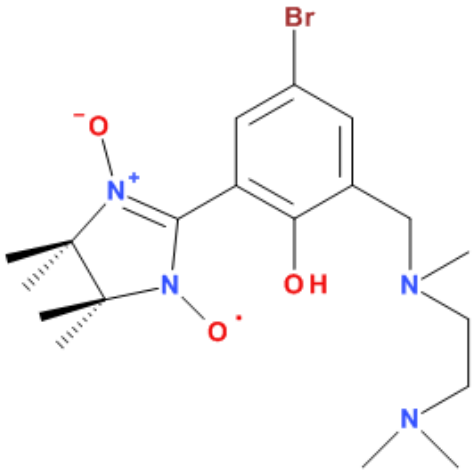

Scheme 1

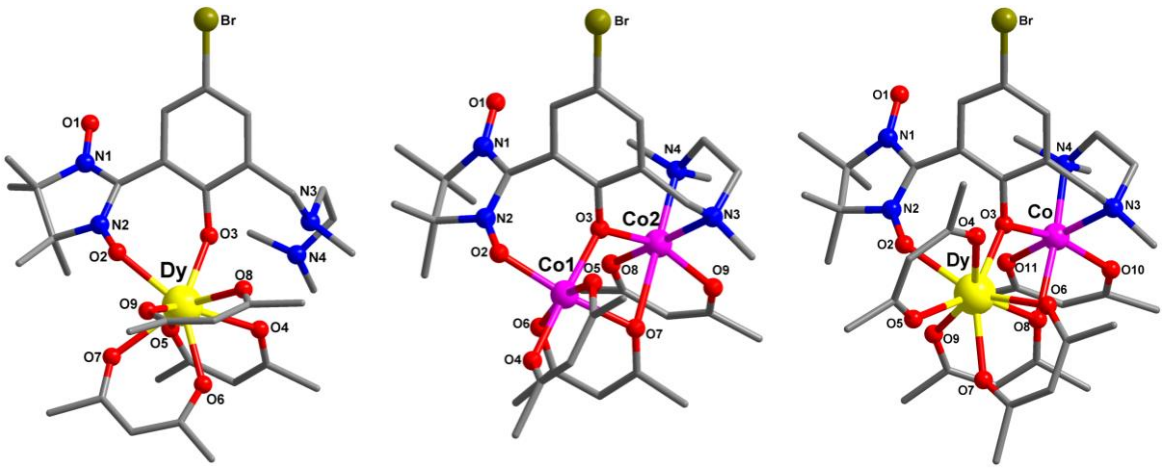

(a) **(b)** **(c)**

Figure 1. Perspective views of compounds **1**(a), **2** (b), and **3** (c). The hydrogen and fluorine atoms have been omitted for clarity.

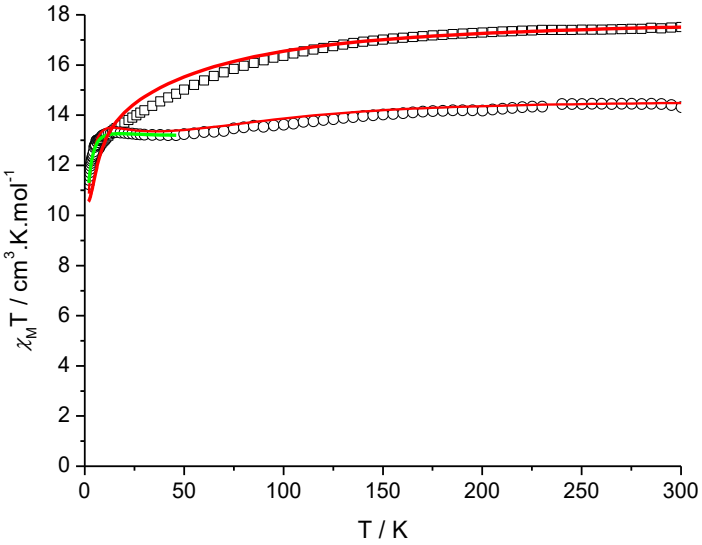

Figure 2. Plots of $\chi_M T$ *vs. T* for compounds **1** (open circle) and **3** (open square), measured at *H* = 1 kOe. The green line corresponds to the best fit for **1** (vide text). The red lines correspond to the best simulations (vide text).

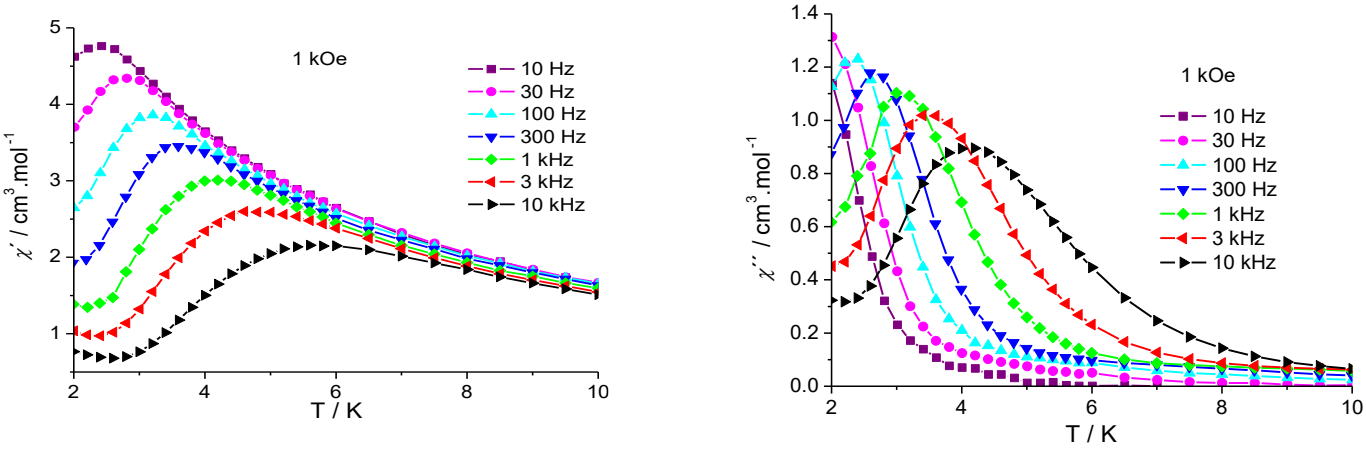

Figure 3. Thermal dependence of the (left) in-phase χ' and (right) out-of-phase χ'' susceptibility components for compound **1** measured under applied H = 1 kOe.

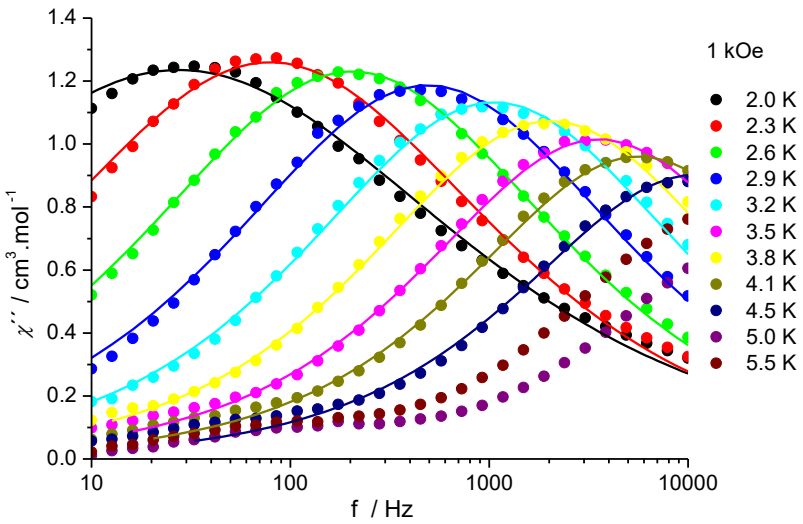

Figure 4. Frequency dependence of the out-of-phase (χ'') components of the ac magnetic susceptibility for compound **1** at H = 1 kOe. Solid lines represent the fits to the data as described in the text.

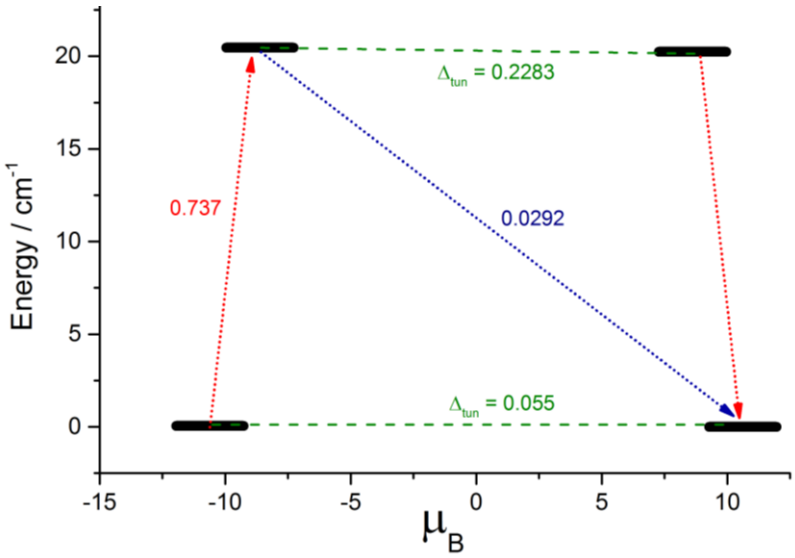

Figure 5. Low lying exchange states and transition moments for **1**. The thick black horizontal lines indicate the Kramers' doublets as a function of the projection of the magnetic moment on the chosen quantisation axis (the one of the ground multiplet). The dotted arrows show the possible pathways of different Orbach processes. The dashed green lines represent the presence of quantum tunnelling between the connecting states. The numbers reported for each arrow are

the mean absolute value for the corresponding matrix element of the transition magnetic moment.

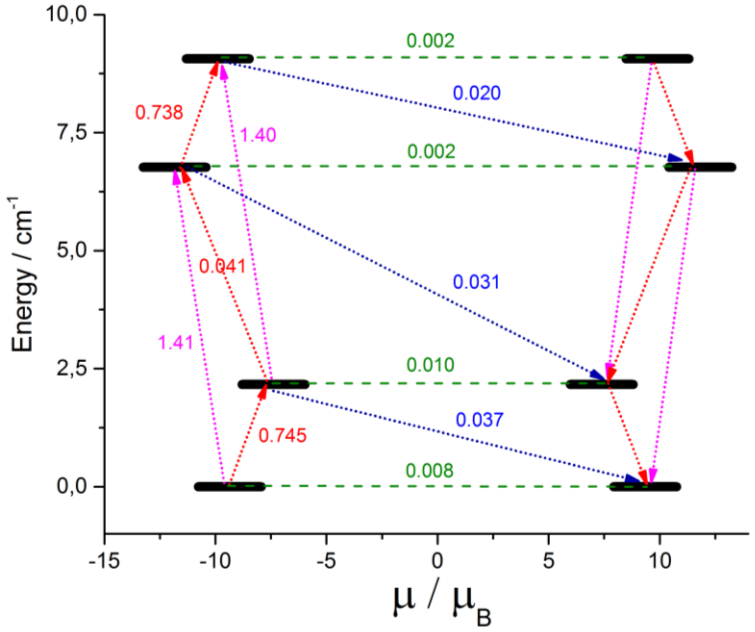

Figure 6. Low lying exchange states and transition moments for **3.** See Figure 5 for the legend.

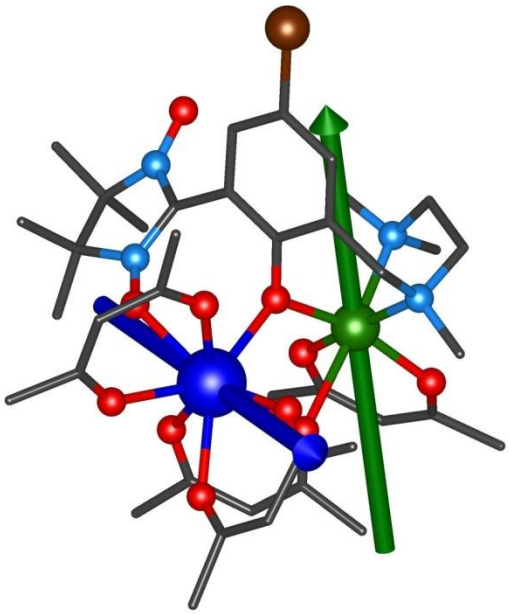

Figure 7. Orientations of the magnetic easy axes for **3**. Dysprosium, cobalt, oxygen, nitrogen, bromine and carbon are blue, green, red, pale blue, brown and grey, respectively. Hydrogen and fluorine atoms are not shown for sake of clarity.

TABLE OF CONTENTS ENTRY

Original end-off bicompartmental ligands bearing a nitronyl-nitroxide arm have been designed for synthesizing various heterospin molecular systems.